Screening of differentially expressed miRNAs in tensile strain-treated HepG2 cells by miRNA microarray analysis

XU LUO[1*], SI SHEN[1*], SUHONG YI[1,2*], JIANGFENG HU[3], YUNCHEN SUN[1], KEWEI GAO[1] and LIANG ZHU[1]

[1]Department of Gastroenterology, Changzheng Hospital, Second Military Medical University,
Shanghai 200003; [2]Department of Gastroenterology, Xinyu People's Hospital, Xinyu, Jiangxi 338000;
[3]Department of Gastroenterology, Shanghai First People's Hospital, Shanghai 200003, P.R. China

Abstract. Cirrhosis and portal hypertension are associated with an increased risk of developing liver cancer. However, it is unknown how changes in the cellular mechanical microenvironment induced by portal hypertension affect the occurrence and development of liver cancer. The aim of this study was to determine the effect of tensile strain on the proliferation of a human liver cancer cell line (HepG2 cells) using methods such as flow cytometry, Cell Counting Kit-8 and 5-bromodeoxyuridine assays, and to examine the changes in microRNA (miRNA/miR) expression using microarray, reverse transcription-quantitative (RT-q)PCR and bioinformatics analyses. It was demonstrated that cyclic tensile force promoted the proliferation of HepG2 cells. The most suitable research conditions were as follows: Tensile strain force loading amplitude 15%; frequency 1 Hz; and time 24 h. After loading the HepG2 cells under such conditions, the differentially expressed miRNAs were screened out using an Agilent Human miRNA Microarray, identifying seven miRNAs with significant differences (expression difference >2 times and $P < 0.05$). A total of five were upregulated, including hsa-miR-296-5p, hsa-miR-6752-5p, hsa-miR-6794-5p, hsa-miR-6889-5p and hsa-miR-7845-5p; and two were downregulated, hsa-miR-4428 and hsa-miR-503-5p. The results of RT-qPCR also further confirmed the expression changes of these miRNAs. Gene Ontology and pathway analyses showed the involvement of these miRNAs in numerous important physiological processes. These findings may provide novel miRNA-based information, thus enhancing the understanding of the pathophysiological processes leading to liver cancer.

Introduction

Hepatitis viruses can cause infections that lead to liver cirrhosis, which then increases the risk of liver cancer; thus, hepatitis-cirrhosis-liver cancer is considered to be a 'trilogy' of events (1). Clinical data have shown that most patients with liver cancer had a background of liver fibrosis or cirrhosis (2). In a previous study, the liver stiffness measurement was evaluated in a group of patients with chronic hepatitis C, it was found that the stiffness of the liver could be an independent risk factor for the occurrence of liver cancer (1). It has also been shown that the higher the degree of hepatic fibrosis, the higher the intrahepatic metastasis rate of liver cancer, indicating a significant association between hepatic fibrosis and proliferation, invasion and metastasis of liver cancer cells (3). An *in vivo* experiment, in which liver cancer cells were injected into mice with induced liver fibrosis, demonstrated that liver fibrosis was associated with the development of tumors in these mice (4).

Cirrhosis of the liver can lead to sinusoidal portal hypertension, in which the pressure in the hepatic portal vein increases, which can cause these veins to become significantly dilated (5). Hepatocytes are epithelial cells that line the sinusoids, which are directly and indirectly affected by biomechanical factors, such as the pressure of the hepatic portal vein and the tension strain after the dilation of hepatic sinusoids (6). A number of studies have shown the important roles of biomechanical factors in the regulation of hepatocyte function. Our previous experiments found that mechanical pressure promotes the proliferation, migration and invasion of liver cancer cells (HepG2 and Huh-7) (7). A total of five pressure-responsive microRNAs (miRNAs/miRs) were screened from the results of the mRNA and miRNA microarray, which were uploaded to the Gene Expression Omnibus database (chip nos. GSE119881

Correspondence to: Dr Liang Zhu, Department of Gastroenterology, Changzheng Hospital, Second Military Medical University, 415 Fengyang Road, Huangpu, Shanghai 200003, P.R. China
E-mail: czzhuliang@smmu.edu.cn

*Contributed equally

and GSE120194). Our previous and present results have both indicated that mechanical stimulation may affect the growth and metastasis of liver cancer (7). Moreover, mechanical stretching has been found to significantly increase the expression of transforming growth factor β (TGF-β) mRNA and related proteins in liver cells (8). In the early stages of portal hypertension, mechanical stretching increased the expression level of matrix metalloproteinase-1 in hepatic stellate cells, reduced the expression levels of tissue inhibitor of metalloproteinases (TIMP)1 and TIMP2, and inhibited the degradation of the extracellular matrix (9). However, the effect of tensile strain on liver cancer cells and its related miRNAs have not yet been reported.

miRNAs are 21-to-23-nucleotide-long noncoding RNA molecules that have important roles in regulating cell proliferation, differentiation and apoptosis (10). Some miRNAs are related to both tensile strain and liver cancer, including miR-29 and miR-21. For example, previous studies demonstrated that the expression of the miR-29 family was downregulated in periodontal ligament cells loaded with tensile strain for 24 h (11) and in liver cancer cells (12). Additionally, the expression of miR-21 in vascular smooth muscle cells (VSMCs) increased significantly after tensile strain loading and in liver cancer tissues (13). These results indicated that certain tension-responsive miRNAs may be important in the development of liver cancer. Therefore, in the present study, the effects of strain force on the proliferation of a human liver cancer cell line (HepG2) were measured by flow cytometry, Cell Counting Kit-8 (CCK-8) and 5-bromodeoxyuridine (BrdU) assays. An Agilent monochromatic marker chip was used to screen differentially expressed miRNAs, and reverse transcription-quantitative (RT-q)PCR was used to verify the results. Gene Ontology (GO) and pathway analyses were used to analyze genes and provide information on how the mechanical microenvironment of liver cancer affects the behavior of liver cancer cells.

The present results suggested that the expression levels of miRNAs in HepG2 cells was significantly changed after loading under the optimal conditions (amplitude of 15% at 1 Hz for 24 h). In total, seven differentially expressed miRNAs and 224 target genes were screened. Among them, SMAD7 and SP1 were further examined, with regards to their related functions and mechanisms. GO and Kyoto Encyclopedia of Genes and Genomes (KEGG) analysis suggested that the biological functions of the target genes were mainly related to various cancer types, including TGF-β/mitogen-PI3K/Akt and other signaling pathways, closely related to different cancer types. Moreover, the possible mechanism was identified to be via the regulation of SMAD7 and TGF-β signaling pathway by hsa-miR-503-5p.

Materials and methods

Cell culture. HepG2 cells were purchased from American Type Culture Collection (cat. no. HB 8065). HL-7702 cells were purchased from cell bank of typical culture preservation Committee of Chinese Academy of Sciences. The cells were cultured at 37°C in an atmosphere containing 5% CO_2 in Dulbecco's modified Eagle's medium (DMEM; Jiangsu Kaiji Biotechnology Co., Ltd.) containing 10% fetal bovine serum

(FBS; Gibco; Thermo Fisher Scientific, Inc.) for different durations (2, 6, 12, 24 and 48 h). The cell line was authenticated by short tandem repeat analysis.

Cyclic stretching device. In this experiment, the FX-4000T™ Tension system (Flexcell International Corporation) purchased by the Biomechanics Laboratory of Shanghai Jiao Tong University was used. The tensile strain principle of the device was to use a vacuum pump to draw air, make space under an elastic film in the vacuum environment and produce downward tension strain. When the vacuum pump was relaxed, the elastic membrane retracted under its own elastic force and circulated, thus producing periodic tensile strain (14).

BioFlex amino-culture plate coating. Numerous routine treatment methods were tested in the laboratory, such as soaking in hydrochloric acid (plate) for 24 h, followed by soaking in water for 24 h, then drying, gelatin coating or cleaning. Moreover, drying after soaking in 75% alcohol for 24 h, then gelatin coating was performed. However, when using these methods cells did not adherent to the wells and grew poorly. Later, the plate was washed and dried. Then, the gelatin was changed into rat tail collagen for coating, it was found that the cells could adhere to the wall and grow efficiently. The BioFlex amino-culture plates (Flexcell International Corporation) were coated with 2 mg/ml rat tail collagen solution (Roche Diagnostics). Then, 20 µl of collagen solution was added to each well and smeared evenly with an aseptic cell scraper. Subsequently, the plates were blow-dried on a clean bench and irradiated with ultraviolet light for 1 h.

Cyclic stretch application. The cells were seeded on BioFlex amino-culture plates at a density of $1x10^5$ cells/well. After 24 h, the culture medium was replaced with serum-free medium for another 24 h to synchronize the cells in 37°C incubator. The cells in the serum-free medium were then exposed to cyclic stretch provided by the FX-4000T Tension system.

Flow cytometry analysis. In the periodic strain-loaded cells, three main parameters were used; these were tensile strain amplitude, tension strain frequency and time. By fixing two of the parameters, the other parameter was changed to observe the effect of tension strain on HepG2 cells (except these three parameters, all the other experimental conditions were the same). After synchronizing HepG2 cells implanted on BioFlex amino-culture plates for 24 h, three groups of experiments were set up: i) Tension strain time (tensile strain frequency fixed to 1 Hz; amplitude to 15%; and tension strain time set to 2, 6, 12, 24 or 48 h, a total of five experimental groups); ii) tensional strain frequency (tensile strain time fixed to 24 h; amplitude to 15%; and tensile strain frequency set to 0.5 and 1 Hz, a total of two experimental groups); and iii) tensile strain amplitude (tensile strain time fixed to 24 h; frequency to 1 Hz; and tensile strain amplitude set to 5 and 15%, a total of two experimental groups). All the control groups were nontension loaded groups. After tension loading, the cells were digested with trypsin (containing EDTA; Jiangsu Kaiji Biotechnology Co., Ltd.), resuspended with 0.5 ml 1X PBS containing 50 µg/ml propidium iodide (PI) and 200 µg/ml ribonuclease (Roche Diagnostics) and incubated

Table I. Primer design.

Gene name	Primer sequence (5'→3')	
hsa-miR-7845-5p	F: GCGAAGGGACAGGGAGGG	
	R: AGTGCAGGGTCCGAGGTATT	
	RT primer: GTCGTATCCAGTGCAGGGTCCGAGGTATTCGCACTGGATACGACCCACGA	
hsa-miR-6889-5p	F: GTCGGGGAGTCTGGGGTC	
	R: AGTGCAGGGTCCGAGGTATT	
	RT primer: GTCGTATCCAGTGCAGGGTCCGAGGTATTCGCACTGGATACGACATTCCG	
hsa-miR-6794-5p	F: CGCAGGGGGACTGGGG	
	R: AGTGCAGGGTCCGAGGTATT	
	RT primer: GTCGTATCCAGTGCAGGGTCCGAGGTATTCGCACTGGATACGACGCTCAC	
hsa-miR-6752-5p	F: GGGGGGTGTGGAGCCA	
	R: AGTGCAGGGTCCGAGGTATT	
	RT primer: GTCGTATCCAGTGCAGGGTCCGAGGTATTCGCACTGGATACGACGCCCCC	
hsa-miR-503-5p	F: CGTAGCAGCGGGAACAGTT	
	R: AGTGCAGGGTCCGAGGTATT	
	RT primer: GTCGTATCCAGTGCAGGGTCCGAGGTATTCGCACTGGATACGACCTGCAG	
hsa-miR-4428	F: CGCAAGGAGACGGGAACA	
	R: AGTGCAGGGTCCGAGGTATT	
	RT primer: GTCGTATCCAGTGCAGGGTCCGAGGTATTCGCACTGGATACGACGCTCCA	
hsa-miR-296-5p	F: GAGGGCCCCCCCTCAA	
	R: AGTGCAGGGTCCGAGGTATT	
	RT primer: GTCGTATCCAGTGCAGGGTCCGAGGTATTCGCACTGGATACGACACAGGA	
U6	F: GCTTCGGCAGCACATATACTAAAAT	
	R: CGCTTCACGAATTTGCGTGTCAT	
	RT primer: CGCTTCACGAATTTGCGTGTCAT	

F, forward; R, reverse; miR, microRNA; RT, reverse transcription.

at 37˚C for 30 min. PI is an insertion nucleic acid fluorescent dye; its binding amount is proportional to the content of DNA in the cell. Using flow cytometry and FlowJo V10 software (FlowJo LLC) DNA distribution status at various stages of the cell cycle can be obtained, and the percentage of each cell cycle can be calculated. After propidium iodide staining, if the fluorescence intensity of G0/G1 phase cells is 1, the theoretical value of the fluorescence intensity of G2/M phase cells that contain double genomic DNA is 2, and the fluorescence intensity of S phase cells undergoing DNA replication is 1-2 (15). Then, flow cytometry was used to detect the cell cycle with a standard program. In the analysis, the proliferation index $(PI) = (S + G2/M) / (G0/G1 + S + G2/M)$ was used to evaluate the effect of different tensile strain loading conditions on cell proliferation, and the ideal tension strain conditions for HepG2 cells were determined. The experiment was repeated three times.

BrdU assay. The HepG2 cells and HL-7702 cells seeded on the BioFlex amino-culture plates were synchronized for 24 h and then connected to the Flexcell FX-4000T Tension system. The experimental group was treated for 24 h with a tensile strain amplitude of 15% and a frequency of 1 Hz, while the control group was the non-tension loaded group.

BrdU (2 μl/well; Sigma-Aldrich; Merck KGaA) was added to the tension strain and control groups simultaneously at 8 h before the end of the tension strain treatment in the 37˚C incubator. At the end of the strain, the cells were collected by trypsin digestion, and the cell concentration was adjusted to $1x10^5$/ml in DMEM (containing 10% FBS). The cells were cultured on the 96-cell plate (100 μl of cell suspensions/well) at 37˚C in an atmosphere containing 5% CO_2 for 4 h until they adhered. Finally, the medium was dried and put in a 4˚C refrigerator overnight. Furthermore, FixDenat solution (200 μl/well; Sigma-Aldrich; Merck KGaA) was added and incubated for 30 min at room temperature. The anti-BrdU-Peroxidase storage solution was diluted 100 times with antibody diluent, added to the cells (100 μl/well) and incubated at room temperature for 90 min. The supernatant was removed, and PBS was used to wash the cells three times. Next, tetramethylbenzidine substrate (100 μl/well; Sigma-Aldrich; Merck KGaA) was added at room temperature for 5-30 min to complete color development. Subsequently, sulfuric acid (1 M) was added to terminate the reaction immediately (25 μl/well). The 96-cell plate was vibrated for 60 sec and the absorbance was measured at 450 nm using a microplate reader (Bio-Rad Laboratories, Inc.), with a reference wavelength of 630 nm.
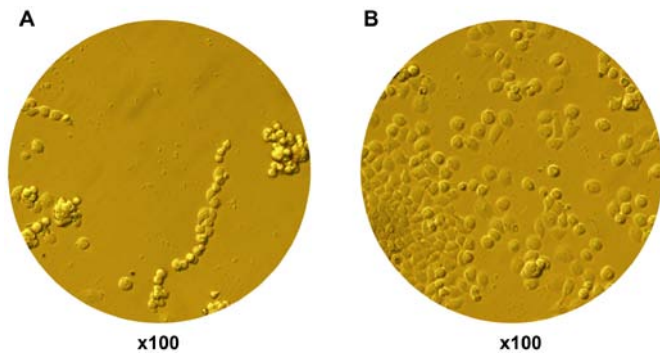
Figure 1. Increase in cell adherence and growth using collagen coating. (A) Collagen-free coating (magnification, x100). (B) Collagen coating (magnification, x100).

CCK-8 assay. The HepG2 cells seeded on the BioFlex amino-culture plates were synchronized for 24 h and then connected to the Flexcell FX-4000T Tension system. The experimental group was treated for 24 h with a tensile strain amplitude of 15% and a frequency of 1 Hz, while the control group was the nontension loaded group. Then, 0.5 h before the end of the tension strain treatment, CCK-8 reagent (Sangon Biotech, Co., Ltd.) was added to the tension strain and control groups at the same time (200 μl/well), and the assay was operated according to the manufacturer's protocols. After the tension strain treatment, the cell culture medium in each well was transferred into a 96-well plate. Subsequently, the 96-cell plate was put in the microplate reader (Bio-Rad Laboratories, Inc.). After vibration for 60 sec, the absorbance at 450 nm was measured, with a reference wavelength of 630 nm.

miRNA expression analysis using a miRNA array. Total RNA was extracted by TRIzol® reagent (Thermo Fisher Scientific, Inc.) according to the manufacturer's protocol, purified using miRNeasy Mini kit (Qiagen GmbH) and quantified using the NanoDrop™ 2000 (Thermo Fisher Scientific, Inc.), and the RNA integrity was assessed using an Agilent 2100 Bioanalyzer instrument (Agilent Technologies, Inc.). The sample labeling, microarray hybridization and washing were performed based on the manufacturer's standard protocols. Differentially expressed miRNAs were then identified based on fold-change and P-value, as calculated using the t-test. The threshold set for up- and downregulated genes was a fold-change ≥2.0 and P<0.05.

RT-qPCR. RT-qPCR was performed to validate the microarray data. The extracted total RNAs were reverse transcribed using Moloney Murine Leukemia Virus reverse transcriptase (Thermo Fisher Scientific, Inc.) with a special stem-loop primer (RT primer). The thermocycling conditions were as follows: 42°C for 1 h, followed by 70°C for 5 min. Then, RT-qPCR was performed with a SYBR Green PCR kit (Takara Bio, Inc.) on an ABI PRISM 7500 Real-time PCR system (Applied Biosystems; Thermo Fisher Scientific, Inc.) according to the manufacturer's protocols. The thermocycling conditions were as follows: Initial denaturation at 95°C for 15 min, followed by 40 cycles at 62°C for 40 sec, 95°C for 1 min and 55°C for 1 min. The sequences of RT and PCR primers are listed in Table I. The expression levels of miRNAs were normalized to U6 expression. miRNA expression levels were calculated using the $2^{-\Delta\Delta Cq}$ method (16).

Target genes of differentially expressed miRNAs. Target genes of differentially expressed miRNAs were determined as the intersection of the predictions of the three databases: TargetScan V7.2 (http://www.targetscan.org/), microRA.org (http://www.microrna.org; November 2010 version) and PITA (https://genie.weizmann.ac.il/) (17). All data were obtained from the databases in January 2019.

GO and pathway analyses of predicted mRNA targets. GO analysis (http://geneontology.org/docs/go-citation-policy/) and pathway analysis were performed on predicted mRNA targets of miRNAs using Database for Annotation, Visualization, and Integrated Discovery (18) and KEGG database (19,20), respectively. Specific biological process categories and pathways were enriched. The threshold of significance was defined by P<0.05 and Benjamini-Hochberg (21) false discovery rate (FDR-bh) <0.25.

Statistical analysis. Statistical analysis was performed using GraphPad Prism 6 software (GraphPad Software, Inc.). Each experiment was performed at least three times, and all values were expressed as the mean ± standard deviation. Data from ≥3 were analyzed using one-way ANOVA followed by Fisher's Least Significant Difference or Dunnett's post hoc comparison test as applicable. P<0.05 was considered to indicate a statistically significant difference.

Results

BioFlex amino-culture plate coating. Due to the lack of related reports on HepG2 cells cultured on BioFlex plates, several methods were tried in this experiment. Finally, type I rat tail collagen was selected. The results showed that type I rat tail collagen coating led to increased cell adherence and growth of HepG2 cells in the BioFlex plates (Fig. 1).

Using flow cytometry to determine the most suitable strain condition. i) Tension strain time: The PI increased significantly in 24 and 48 h groups compared with the control group without tension (P<0.0001; Fig. 2A and B). ii) Tensional strain frequency: The PI increased significantly in the 1 Hz group compared with the control group without tension (P<0.001; Fig. 2C and D). iii) Tensile strain amplitude: The PI increased significantly in the 15% group compared with the control group without tension (P<0.0001; Fig. 2E and F).

Based on the experimental results of the aforementioned three groups of tensile strain loading conditions, a tensile strain amplitude of 15%, frequency of 1 Hz and time of 24 h were selected as the ideal conditions for the following experiments.

Proliferation of liver cancer cells is promoted by tensor strain. The results of the BrdU assay showed that the tensile strain amplitude of 15% at 1 Hz for 24 h significantly promoted DNA synthesis in cells compared with the control group (P<0.001; Fig. 3A). Additionally, the CCK-8 assay also demonstrated that these conditions significantly promoted DNA synthesis in
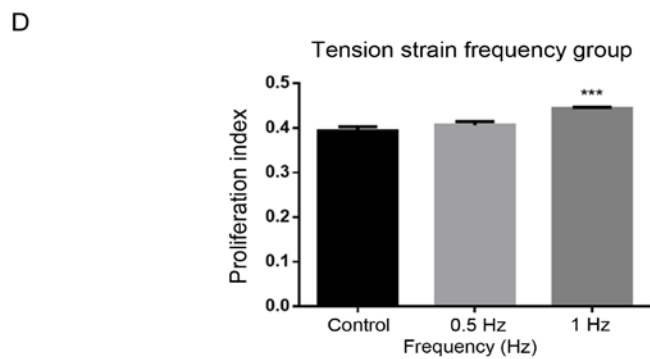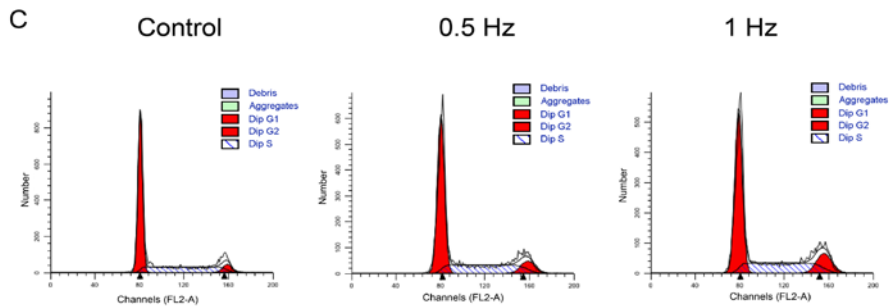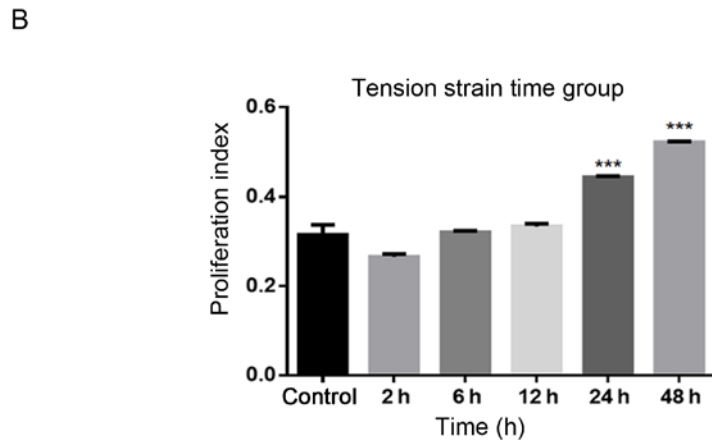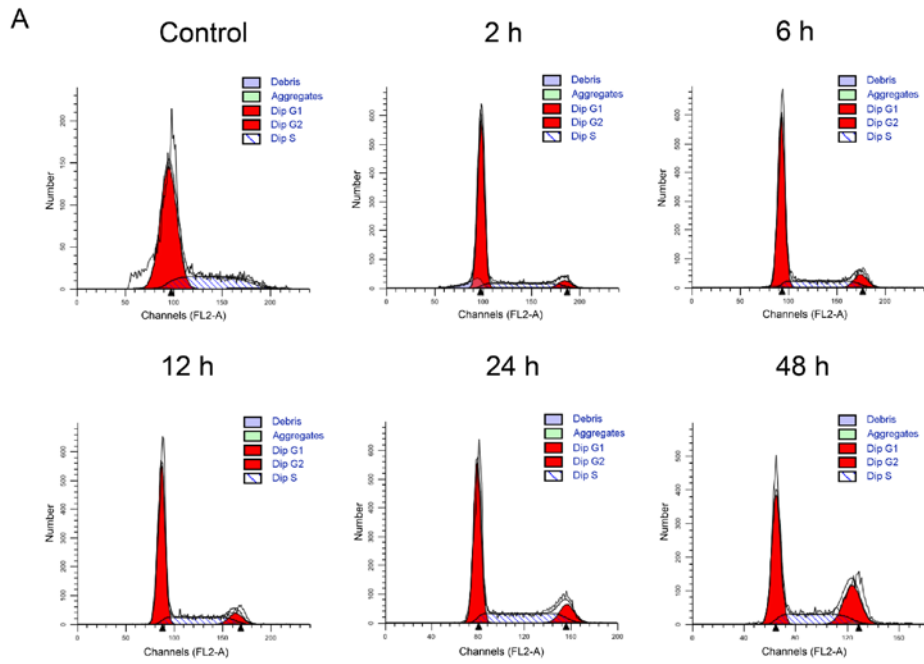
Figure 2. Determination of the most suitable strain condition using flow cytometry. (A) Time group: (B) Compared with the control group without tension, the PI increased significantly in 24 h and 48 h groups. (C) Frequency group: (D) Compared with the control group without tension, the PI increased significantly in 1 Hz group.
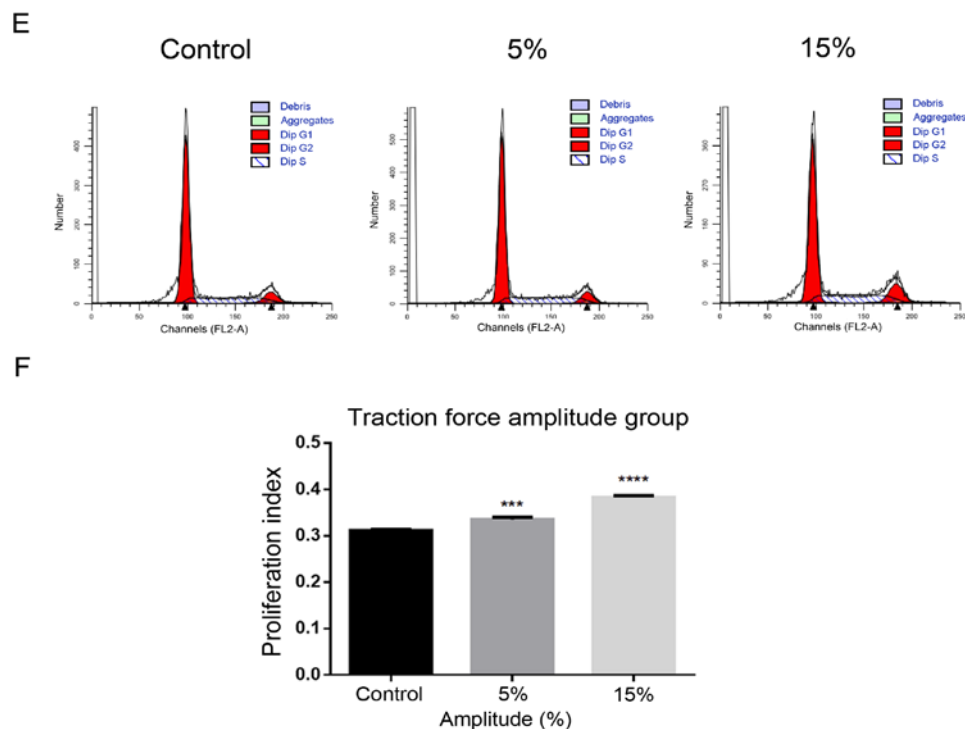
Figure 2. Continued. Determination of the most suitable strain condition using flow cytometry. (E) Amplitude group: (F) Compared with the control group without tension, the PI increased significantly in the 5 and 15% groups. All the control groups were non-tension loaded groups. The data of PI are shown as the mean ± SD from three wells/group. ***P<0.001, ****P<0.0001 vs. control. PI, proliferation index.
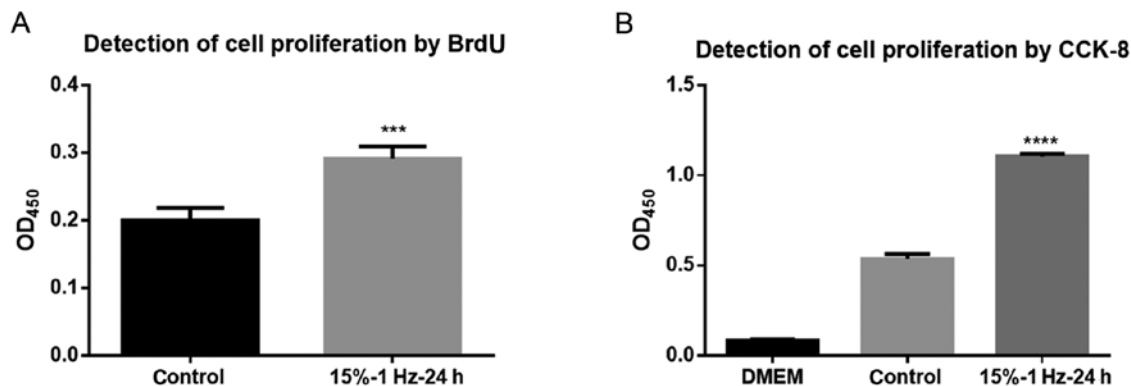

Figure 3. Measuring cell proliferation. (A) BrdU assay demonstrated that tensor strain promotes cell proliferation. The results showed that compared with the control group, the tensile strain amplitude of 15% and the frequency of 1 Hz for 24 h significantly promoted the DNA synthesis of the cells. (B) CCK-8 assay indicated that tensor strain promotes cell proliferation. The results showed that compared with the control group, the tensile strain amplitude of 15% and the frequency of 1 Hz for 24 h significantly promoted the DNA synthesis of the cells. ***P<0.001, ****P<0.0001 vs. control. BrdU, 5-bromodeoxyuridine; CCK-8, Cell Counting Kit-8; OD, optical density.

the cells (P<0.0001; Fig. 3B). Thus, this indicated that tensile strain could lead to increased liver cancer cell proliferation.

Differentially expressed miRNAs in response to tensile strain. To investigate the effects of tensile strain on the miRNA profile of HepG2 cells, tensile strain was applied to the activated HepG2 cells, and RNA was extracted and subjected to microarray analysis. As shown in Table II, seven significantly differentially expressed miRNAs showed a fold-change threshold of ≥2.0 and P<0.05. Of these seven miRNAs in the tensile strain-treated group, five were upregulated (hsa-miR-296-5p, hsa-miR-6752-5p, hsa-miR-6794-5p, hsa-miR-6889-5p and hsa-miR-7845-5p) and two were down-

regulated (hsa-miR-4428 and hsa-miR-503-5p) compared with the control group.

Validation of miRNA microarray with RT-qPCR. RT-qPCR was performed to validate the microarray results of the five upregulated and two downregulated miRNAs. As shown in Fig. 4, the changes in the seven miRNAs detected by RT-qPCR were consistent with those of the miRNA microarray.

GO and KEGG pathway analyses. Potential target genes for the aforementioned seven differentially expressed miRNAs were searched using three bioinformatics databases, miRNAorg, PITA and TargetScan, which predicted

Table II. Differentially expressed miRNAs.

miRNA	P-value	Regulation	FC
hsa-miR-296-5p	0.00094	up	6.387268
hsa-miR-4428	0.015763873	down	-2.8974507
hsa-miR-503-5p	0.043706737	down	-4.2659197
hsa-miR-6752-5p	0.015388427	up	9.723028
hsa-miR-6794-5p	0.000131	up	20.911135
hsa-miR-6889-5p	0.027508989	up	11.433076
hsa-miR-7845-5p	0.000946	up	9.37658

miRNA/miR, microRNA.

Table III. Predictive target genes for differentially expressed miRNAs.

miRNA	Predictive target genes
hsa-miR-296-5p	2,613
hsa-miR-4428	3,043
hsa-miR-6752-5p	2,572
hsa-miR-6794-5p	2,521
hsa-miR-6889-5p	1,279
hsa-miR-7845-5p	2,327
hsa-miR-503-5p	1,850
Total	16,205

miR/miRNA, microRNA.

Figure 5. Results of database analysis. In order to remove the false results, the intersection of three databases were taken for 224 target genes.
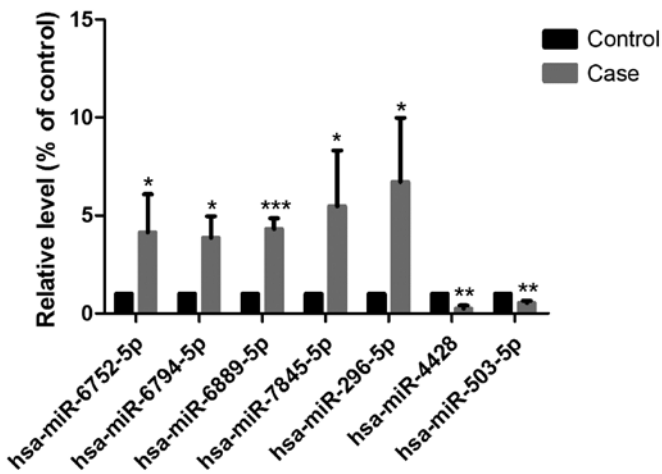

Figure 4. Changes in expression levels of seven miRNAs detected by RT-qPCR. Results of RT-qPCR are consistent with those of the miRNA microarray. *P<0.05, **P<0.01, ***P<0.001 vs. control. miR/miRNAs, microRNAs; RT-qPCR, reverse transcription-quantitative PCR.

2,306, 1,277 and 16,205 target genes, respectively. The false results were removed by taking the intersection of the results from the three databases for 224 target genes (Fig. 5). The 16,205 predi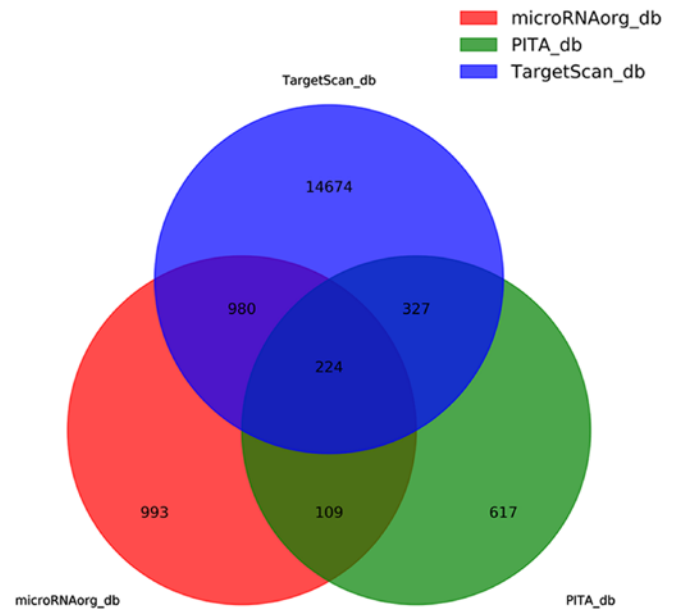ctive target genes refer to the sum of all seven predictive target genes that differentially express miRNAs. The components are shown in the Table III.

GO and pathway analyses were used to understand the biological characteristics of the aforementioned target genes. Using a threshold of FDR-bh <0.25, 132 GO terms were considered to be significant. Additionally, 6, 25 and 101 GO terms belonged to the 'cellular component' category (Fig. 6A), 'molecular function' category (Fig. 6B) and 'biological process' category (Fig. 6C), respectively. The x-axis of Fig. 6 shows the P-value corrected by FDR-bh algorithm, which is converted by -log10. The longer the column is, the higher the enrichment degree is. The target genes were concentrated in 'cyclin-dependent protein kinase holoenzyme complex', 'neuromuscular junction', 'microtubule cytoskeleton', 'protein kinase binding', 'protein binding', 'positive regulation of transcription from RNA polymerase II promoter', 'positive regulation of transcription, DNA-templated', 'negative regulation of cell migration', 'positive regulation of skeletal muscle tissue development' and 'patterning of blood vessel' categories.

Using KEGG pathway analysis, 52 significant KEGG pathways were identified at a cutoff FDR-bh <0.25. These pathways included diseases, such as 'breast cancer', 'melanoma', 'prostate cancer', 'endocrine resistance' and 'bladder cancer', and signaling pathways, such as 'mitogen-activated protein kinase (MAPK) signaling pathway', 'PI3K-Akt signaling pathway', 'forkhead box O signaling pathway' and 'Ras signaling pathway' (Fig. 6D).

Strain has no effect on the proliferation of normal liver cells. Using BrdU experiments, it was demonstrated that the proliferative ability of HepG2 cells after tension intervention was significantly improved (P<0.05), while the proliferative ability of normal hepatocyte HL-7702 did not change significantly (Fig. 7).

Flexcell-5000T was also used to performed traction experiments on Huh-7 cells and MHCC97H cells, but the two cells
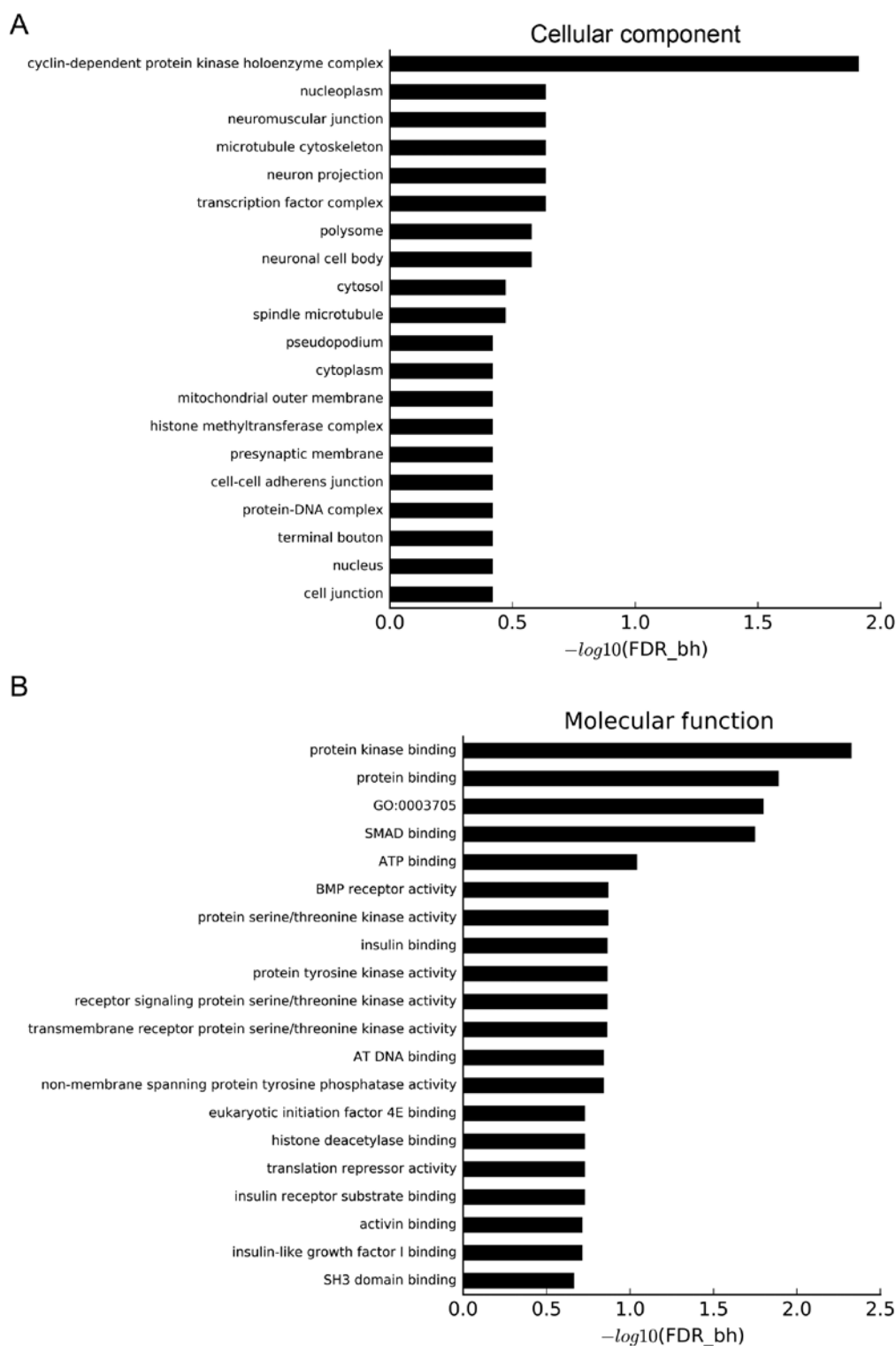
Figure 6. GO and KEGG analyses. GO analysis based on miRNA-targeted genes using three databases: (A) 'Cellular component' category; and (B) 'molecular function' category.

could not adhere to the membrane on the traction plate, and thus HepG2 cells were selected for subsequent experimentation.

Discussion

Human liver cancer cells grow in a complex internal environment where the mechanical factors should not be ignored.

The present study demonstrated that tensile strain promoted the growth of liver cancer cells and accelerated their proliferation. To some extent, this could explain why cirrhosis can significantly increase the occurrence and development of liver cancer, but the exact underlying mechanism is still unclear. It has been suggested that other biomechanical forces, such as fluid shear stress, may affect the cytoskeleton of liver cancer cells (22). Subsequently, this fluid shear stress could activate
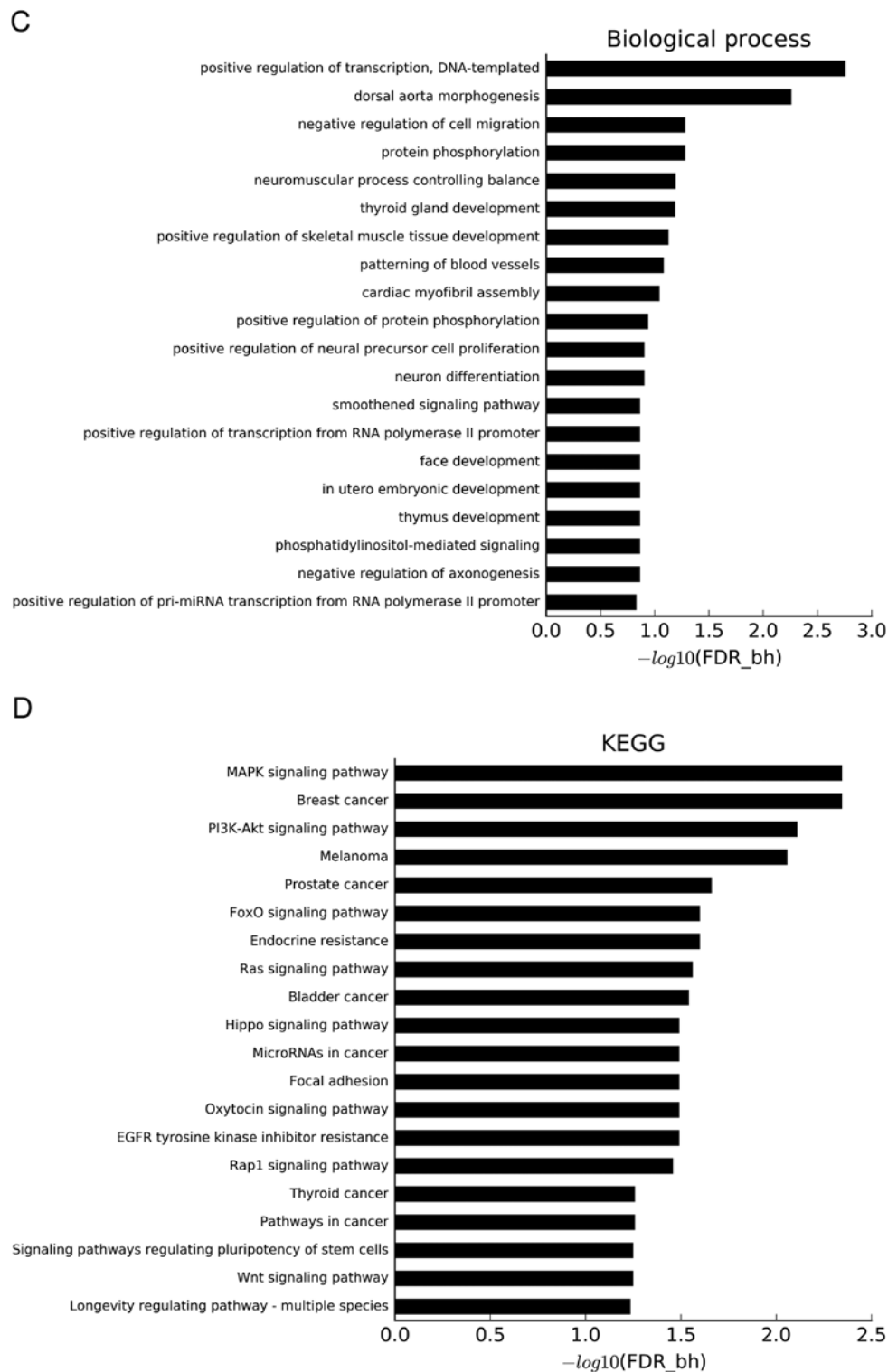
C

D

Figure 6. Continued. GO and KEGG analyses. GO analysis based on miRNA-targeted genes using three databases: (C) 'Biological process' category. (D) Pathway analysis based on miRNA-targeted genes using KEGG. miRNA, microRNA; KEGG, Kyoto Encyclopedia of Genes and Genomes; GO, Gene Ontology; FDR-bh, Benjamini-Hochberg false discovery rate.

signaling pathways, affect the gene expression and influence cellular features (23). Numerous studies have shown that strain can promote the proliferation of various types of cells, such as VSMCs (24), osteoblasts (25) and dermal keratinocytes (26). In the present study, type I rat tail collagen was chosen to coat BioFlex plates for effective adherence and cell growth. Then, suitable tensile strain loading conditions were identified for

human liver cancer cell line HepG2, and seven differentially expressed miRNAs were screened after tensile strain loading.

Previous studies have shown that miR-296-5p is upregulated and plays a role in the progression of various tumors, such as esophageal and laryngeal cancer (27-29). Additionally, it is also overexpressed in a number of tumor cells and induces carcinogenesis in human cells by downregulating the p53-p21
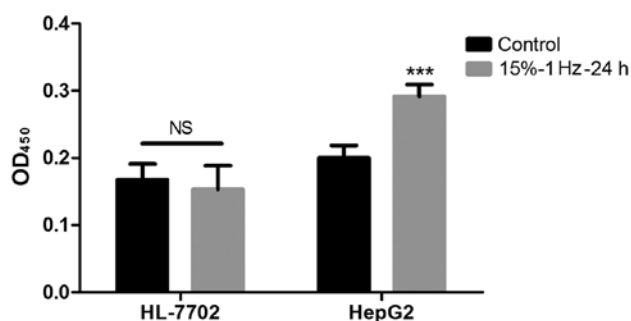
Figure 7. BrdU assay results on proliferative ability of HepG2 cells and normal hepatocyte HL-7702 cells. The proliferation ability of HL-7702 cells was not significantly altered after being coated by strain, but that of HepG2 cells was increased. ***$P<0.001$ vs. control.

(wild-type p53 activated fragment 1) pathway (30). It has been demonstrated that miR-6889-5p has a catalytic role in type 1 autoimmune liver disease (31). It can also inhibit the proliferation of human cells (32). miR-4428 is associated with malignant B-cell lymphoma (33). These previous results suggest that a number of differentially expressed miRNAs are closely related to the development of cancer.

In the present study, it was shown that miR-503-5p was downregulated in tensile strain-treated HepG2 cells. Previous reports have indicated that miR-503-5p is related to the proliferation and invasion of various cancer cells. For example, as a cell migration and invasion suppressor, miR-503-5p can inhibit the metastasis of ovarian cancer cells by inhibiting the CD97-mediated Janus kinase 2/STAT3 pathway (34). It was recently found to inhibit cell epithelial-to-mesenchymal transition and metastasis of liver cancer by inhibiting WEE1 G2 checkpoint kinase, thus predicting the prognosis of liver cancer (35). As a cell proliferation suppressor, miR-503-5p inhibited the proliferation of T24 and EJ bladder cancer cells by interfering with the retinoblastoma gene/E2F signaling pathway (36). However, whether miR-503-5p affects the growth of liver cancer cells by regulating their proliferation has not yet been reported, and it is worth further study. It is worth noting that SMAD7, as one of the target genes of miR-503-5p, is closely related to the expression of TGF-β. TGF-β is a key factor in the process of hepatic fibrosis (8). Previous studies have demonstrated that SMAD7 has roles in various types of cancer; it is overexpressed in endometrial carcinoma (37), it can enhance the tumorigenicity of pancreatic cancer (38) and it is closely associated with colon cancer (39). miR-92b (40) and long noncoding RNA snail family zinc finger 3-antisense 1 (41) could promote liver cancer proliferation and metastasis by targeting SMAD7. These results suggested that mechanical factors may have a biological role by regulating the expression of SMAD7 gene in the development of liver cancer. The specific mechanism underlying this process needs to be identified and studied further.

To understand the specific function of the differentially expressed miRNAs, the target mRNAs of the differentially expressed miRNAs were also analyzed by GO analysis. The results showed that the target mRNAs were involved in numerous physiological processes, including 'cyclin-dependent protein kinase holoenzyme complex', which could indicate that they may exert an anticancer effect by inhibiting the effect of this

complex (42). Furthermore, the genes were enriched in 'transcription factor complex', 'positive regulation of transcription from RNA polymerase II promoter' and 'positive regulation of transcription, DNA templated', which are also related to the DNA transcription and RNA translation of the cells, indicating that the function of miRNAs is closely related to the proliferation and viability of cancer cells. Also, enrichment in 'patterning of blood vessels' may be associated with tumor cells stimulating angiogenesis to provide nutrition. To reveal the regulation of pathways by these miRNAs, KEGG pathway analysis was performed based on the predicted target mRNAs of these miRNAs. Notably, some pathways related to cancers, such as 'breast cancer', 'melanoma', 'prostate cancer' and 'bladder cancer', were identified as significant. The significant 'MAPK signaling pathway' has been reported to be associated with multiple cancers (43-45). Also, 'PI3K-Akt signaling pathway' components were found to be frequently altered in human cancers (46). The results suggested that these pathways might be involved in the proliferation and development of liver cancer, but the specific mechanisms need to be further explored.

In conclusion, a series of changes in tensile strain-treated HepG2 cells were explored in this study. Tensile strain was found to promote the proliferation of HepG2 cell line. Some differentially expressed miRNAs were screened, and their possible target genes and related pathways were preliminarily discussed. There were two major limitations of this research. The first one is that only a single cell line was used in this study. The second is that no experiments were performed to confirm these findings with liver cancer tissues, such as small RNA-seq datasets of low degree hepatic fibrosis and a high degree of hepatic fibrosis liver cancer samples. The follow-up studies may need to be completed by other research groups. The findings could provide new information for the study of carcinogenesis and development of liver cancer and contribute to improving the outcomes for patients with liver cancer.

Availability of data and materials

The datasets used and/or analyzed during the current study are available from the corresponding author on reasonable request.

Authors' contributions

XL, SS, SY and LZ conceived the study, performed the research and wrote the first draft. JH, YS, KG and LZ collected and analyzed the data. All authors contributed to the design and interpretation of the study, and to further drafts. LZ was the guarantor and made substantial contributions to conception and design of the study, and the interpretation of data. LZ supervised and reviewed the results of the experiment and all aspects of the research work and revised the content of the

manuscript prior to submission. All authors read and approved the final manuscript.

Ethics approval and consent to participate

Not applicable.

Patient consent for publication

Not applicable.

Competing interests

The authors declare that they have no competing interests.

Authors' information

LZ is a professor of the Second Affiliated Hospital of the Second Military Medical University, a member of the Shanghai Biomechanics Professional Committee and a peer-reviewed expert of the National Natural Science Foundation of China (NSFC). His main research direction is biomechanical study of digestive system diseases and tumors, with emphasis on liver hemodynamics and gastrointestinal dynamics. For numerous years, our team performed research into the hemodynamics of portal hypertension before and after TIPS, and completed the NSFC project: The role and mechanism of microRNAs in the biomechanical response of hepatic stellate cells. The research reported by this manuscript is one part of another NSFC project: The role of microRNAs regulating the differentiation and invasion of liver cancer in response to mechanical force.

References

1. Masuzaki R, Tateishi R, Yoshida H, Goto E, Sato T, Ohki T, Imamura J, Goto T, Kanai F, Kato N, et al: Prospective risk assessment for liver cancer development in patients with chronic hepatitis C by transient elastography. Hepatology 49: 1954-1961, 2009.
2. Fattovich G, Stroffolini T, Zagni I and Donato F: Hepatocellular carcinoma in cirrhosis: Incidence and risk factors. Gastroenterology 127 (Suppl 1): S35-S50, 2004.
3. Osada S, Kanematsu M, Imai H, Goshima S and Sugiyama Y: Hepatic fibrosis influences the growth of liver cancer. Hepatogastroenterology 55: 184-187, 2008.
4. Kornek M, Raskopf E, Tolba R, Becker U, Klöckner M, Sauerbruch T and Schmitz V: Accelerated orthotopic liver cancers growth is linked to increased expression of pro-angiogenic and prometastatic factors in murine liver fibrosis. Liver Int 28: 509-518, 2008.
5. Qi F, Hu JF, Liu BH, Wu CQ, Yu HY, Yao DK and Zhu L: miR-9a-5p regulates proliferation and migration of hepatic stellate cells under pressure through inhibition of Sirt1. World J Gastroenterol 21: 9900-9915, 2015.
6. Yi S, Qin X, Luo X, Zhang Y, Liu Z and Zhu L: Identification of miRNAs associated with the mechanical response of hepatic stellate cells by miRNA microarray analysis. Exp Ther Med 16: 1707-1714, 2018.
7. Shen S, Luo X, Gao K, Sun Y, Yao D and Zhu L: Identification and integrative analysis of microRNAs and mRNAs involved in proliferation and invasion of pressure treated human liver cancer cell lines. Mol Med Rep 20: 375-387, 2019.
8. Sakata R, Ueno T, Nakamura T, Ueno H and Sata M: Mechanical stretch induces TGF-beta synthesis in hepatic stellate cells. Eur J Clin Invest 34: 129-136, 2004.
9. Goto T, Mikami KI, Miura K, Ohshima S, Yoneyama K, Nakane K, Watanabe D, Otaka M and Watanabe S: Mechanical stretch induces matrix metalloproteinase 1 production in human hepatic stellate cells. Pathophysiology 11: 153-158, 2004.
10. Kozomara A, Birgaoanu M and Griffiths-Jones S: miRBase: From microRNA sequences to function. Nucleic Acids Res 47 (D1): D155-D162, 2019.
11. Chen Y, Mohammed A, Oubaidin M, Evans CA, Zhou X, Luan X, Diekwisch TG and Atsawasuwan P: Cyclic stretch and compression forces alter microRNA-29 expression of human periodontal ligament cells. Gene 566: 13-17, 2015.
12. Parpart S, Roessler S, Dong F, Rao V, Takai A, Ji J, Qin LX, Ye QH, Jia HL, Tang ZY, et al: Modulation of miR-29 expression by α-fetoprotein is linked to the liver cancer epigenome. Hepatology 60: 872-883, 2014.
13. Ladeiro Y, Couchy G, Balabaud C, Bioulac-Sage P, Pelletier L, Rebouissou S and Zucman-Rossi J: MicroRNA profiling in hepatocellular tumors is associated with clinical features and oncogene/tumor suppressor gene mutations. Hepatology 47: 1955-1963, 2008.
14. Vanderploeg EJ, Imler SM, Brodkin KR, García AJ and Levenston ME: Oscillatory tension differentially modulates matrix metabolism and cytoskeletal organization in chondrocytes and fibrochondrocytes. J Biomech 37: 1941-1952, 2004.
15. Davies D and Allen P: DNA Analysis by Flow Cytometry. In: Flow Cytometry. Macey MG (ed). Humana Press, pp165-179, 2007.
16. Livak KJ and Schmittgen TD: Analysis of relative gene expression data using real-time quantitative PCR and the 2-ΔΔCT method. Methods 25: 402-408, 2001.
17. Lewis BP, Shih IH, Jones-Rhoades MW, Bartel DP and Burge CB: Prediction of mammalian microRNA targets. Cell 115: 787-798, 2003.
18. Huang W, Sherman BT and Lempicki RA: Bioinformatics enrichment tools: Paths toward the comprehensive functional analysis of large gene lists. Nucleic Acids Res 37: 1-13, 2009.
19. Yi M, Horton JD, Cohen JC, Hobbs HH and Stephens RM: WholePathwayScope: A comprehensive pathway-based analysis tool for high-throughput data. BMC Bioinformatics 7: 30, 2006.
20. Kanehisa M, Goto S, Kawashima S, Okuno Y and Hattori M: The KEGG resource for deciphering the genome. Nucleic Acids Res 32: D277-D280, 2004.
21. Benjamini Y and Hochberg Y: Controlling the false discovery rate: A practical and powerful approach to multiple testing. J R Stat Soc B 57: 289-300, 1995.
22. Yan Z, Su G, Gao W, He J, Shen Y, Zeng Y and Liu X: Fluid shear stress induces cell migration and invasion via activating autophagy in HepG2 cells. Cell Adhes Migr 13: 152-163, 2019.
23. Wang X, Zhang Y, Feng T, Su G, He J, Gao W, Shen Y and Liu X: Fluid Shear Stress Promotes Autophagy in Hepatocellular Carcinoma Cells. Int J Biol Sci 14: 1277-1290, 2018.
24. de Waard V, Arkenbout EK, Vos M, Mocking AI, Niessen HW, Stooker W, de Mol BA, Quax PH, Bakker EN, VanBavel E, et al: TR3 nuclear orphan receptor prevents cyclic stretch-induced proliferation of venous smooth muscle cells. Am J Pathol 168: 2027-2035, 2006.
25. Weyts FA, Bosmans B, Niesing R, van Leeuwen JP and Weinans H: Mechanical control of human osteoblast apoptosis and proliferation in relation to differentiation. Calcif Tissue Int 72: 505-512, 2003.
26. Nishimura K, Blume P, Ohgi S and Sumpio BE: The effect of different frequencies of stretch on human dermal keratinocyte proliferation and survival. J Surg Res 155: 125-131, 2009.
27. Hong L, Han Y, Zhang H, Li M, Gong T, Sun L, Wu K, Zhao Q and Fan D: The prognostic and chemotherapeutic value of miR-296 in esophageal squamous cell carcinoma. Ann Surg 251: 1056-1063, 2010.
28. Maia D, de Carvalho AC, Horst MA, Carvalho AL, Scapulatempo-Neto C and Vettore AL: Expression of miR-296-5p as predictive marker for radiotherapy resistance in early-stage laryngeal carcinoma. J Transl Med 13: 262, 2015.
29. Vaira V, Faversani A, Dohi T, Montorsi M, Augello C, Gatti S, Coggi G, Altieri DC and Bosari S: miR-296 regulation of a cell polarity-cell plasticity module controls tumor progression. Oncogene 31: 27-38, 2012.
30. Yoon AR, Gao R, Kaul Z, Choi IK, Ryu J, Noble JR, Kato Y, Saito S, Hirano T, Ishii T, et al: MicroRNA-296 is enriched in cancer cells and downregulates p21WAF1 mRNA expression via interaction with its 3' untranslated region. Nucleic Acids Res 39: 8078-8091, 2011.
31. Migita K, Komori A, Kozuru H, Jiuchi Y, Nakamura M, Yasunami M, Furukawa H, Abiru S, Yamasaki K, Nagaoka S, et al: Circulating microRNA Profiles in Patients with Type-1 Autoimmune Hepatitis. PLoS One 10: e0136908, 2015.

32. Polioudakis D, Abell NS and Iyer VR: miR-503 represses human cell proliferation and directly targets the oncogene DDHD2 by non-canonical target pairing. BMC Genomics 16: 40, 2015.

33. Jima DD, Zhang J, Jacobs C, Richards KL, Dunphy CH, Choi WW, Au WY, Srivastava G, Czader MB, Rizzieri DA, *et al*; Hematologic Malignancies Research Consortium: Deep sequencing of the small RNA transcriptome of normal and malignant human B cells identifies hundreds of novel microRNAs. Blood 116: e118-e127, 2010.

34. Park GB and Kim D: MicroRNA-503-5p Inhibits the CD97-Mediated JAK2/STAT3 Pathway in Metastatic or Paclitaxel-Resistant Ovarian Cancer Cells. Neoplasia 21: 206-215, 2019.

35. Jiang SP and Li ZR: miR-503-5p regulates cell epithelial-to-mesenchymal transition, metastasis and prognosis of liver cancer through inhibiting WEE1. Eur Rev Med Pharmacol Sci 23: 2028-2037, 2019.

36. Li X, Han X, Yang J, Sun J and Wei P: miR-503-5p inhibits the proliferation of T24 and EJ bladder cancer cells by interfering with the Rb/E2F signaling pathway. Xi Bao Yu Fen Zi Mian Yi Xue Za Zhi 33: 1360-1364, 2017 (In Chinese).

37. Dowdy SC, Mariani A, Reinholz MM, Keeney GL, Spelsberg TC, Podratz KC and Janknecht R: Overexpression of the TGF-beta antagonist Smad7 in endometrial cancer. Gynecol Oncol 96: 368-373, 2005.

38. Kleeff J, Ishiwata T, Maruyama H, Friess H, Truong P, Büchler MW, Falb D and Korc M: The TGF-beta signaling inhibitor Smad7 enhances tumorigenicity in pancreatic cancer. Oncogene 18: 5363-5372, 1999.

39. Broderick P, Carvajal-Carmona L, Pittman AM, Webb E, Howarth K, Rowan A, Lubbe S, Spain S, Sullivan K, Fielding S, *et al*; CORGI Consortium: A genome-wide association study shows that common alleles of SMAD7 influence colorectal cancer risk. Nat Genet 39: 1315-1317, 2007.

40. Zhuang LK, Yang YT, Ma X, Han B, Wang ZS, Zhao QY, Wu LQ and Qu ZQ: MicroRNA-92b promotes liver cancer progression by targeting Smad7 and is mediated by long non-coding RNA XIST. Cell Death Dis 7: e2203, 2016.

41. Li Y, Guo D, Ren M, Zhao Y, Wang X, Chen Y, Liu Y, Lu G and He S: Long non-coding RNA SNAI3-AS1 promotes the proliferation and metastasis of liver cancer by regulating the UPF1/Smad7 signalling pathway. J Cell Mol Med, 2019.

42. Mani S, Wang C, Wu K, Francis R and Pestell R: Cyclin-dependent kinase inhibitors: Novel anticancer agents. Expert Opin Investig Drugs 9: 1849-1870, 2000.

43. Fang JY and Richardson BC: The MAPK signalling pathways and colorectal cancer. Lancet Oncol 6: 322-327, 2005.

44. Kim EK and Choi EJ: Pathological roles of MAPK signaling pathways in human diseases. Biochim Biophys Acta 1802: 396-405, 2010.

45. Ling MT, Wang X, Ouyang XS, Lee TK, Fan TY, Xu K, Tsao SW and Wong YC: Activation of MAPK signaling pathway is essential for Id-1 induced serum independent prostate cancer cell growth. Oncogene 21: 8498-8505, 2002.

46. Fresno Vara JA, Casado E, de Castro J, Cejas P, Belda-Iniesta C and González-Barón M: PI3K/Akt signalling pathway and cancer. Cancer Treat Rev 30: 193-204, 2004.